Journal of Physics: Conference Series **688** (2016) 012126 doi:10.1088/1742-6596/688/1/012126

Relativistic intensity laser interactions with low-density plasmas

L. Willingale[1], P. M. Nilson[2], C. Zulick[1], H. Chen[3], R. S. Craxton[2], J. Cobble[4], A. Maksimchuk[1], P. A. Norreys[5], T. C. Sangster[2], R. H. H. Scott[5], and C. Stoeckl[2]

[1] Center for Ultrafast Optical Science, University of Michigan, 2200 Bonisteel Boulevard, Ann Arbor, Michigan 48109 USA
[2] University of Rochester - Laboratory for Laser Energetics, Rochester, New York 14623, USA
[3] Lawrence Livermore National Laboratory, Livermore, California 94551, USA
[4] Los Alamos National Laboratory, New Mexico, USA
[5] Central Laser Facility, Rutherford Appleton Laboratory, Oxfordshire, UK

E-mail: wlouise@umich.edu

Abstract. We perform relativistic-intensity laser experiments using the Omega EP laser to investigate channeling phenomena and particle acceleration in underdense plasmas. A fundamental understanding of these processes is of importance to the hole-boring fast ignition scheme for inertial confinement fusion. Proton probing was used to image the electromagnetic fields formed as the Omega EP laser pulse generated a channel through underdense plasma. Filamentation of the channel was observed, followed by self-correction into a single channel. The channel radius as a function of time was found to be in reasonable agreement with momentum-conserving snowplough models.

1. Introduction

The highly non-linear interaction of a high-intensity laser propagating through an underdense plasma leads to ponderomotive and relativistic self-focusing [1, 2], filamentation [3, 4], scattering [5], soliton formation [6, 7], channel formation [8, 9] and in extreme conditions complete cavitation [4]. As the laser pulse propagates through an underdense plasma, the ponderomotive force acts to expel the electrons from the regions of highest intensity. A channel, depleted of electrons, forms on the laser propagation axis. The ions, having a much smaller charge-to-mass ratio, are not affected directly by the laser fields, but will move due to the charge separation electric field. The laser sweeps out an approximately cylindrical region, producing a radial electric fields, that accelerates ions in the transverse direction in a Coulomb explosion [10, 11]. The creation of a channel may be used to access the dense fuel core for fast ignition inertial confinement fusion [12], where a laser is used to channel through millimeter-scale underdense plasma [13]. If the ponderomotive force is strong enough, a shock front can propagate out radially, potentially accelerating the ions to higher energies [14] and forming a blast wave [15]. The channel can facilitate Direct Laser Acceleration of the electrons to many times the ponderomotive energy [16, 17, 18, 19] and lead to bright x-ray generation [20].

This experiment combined a relatively long pulse length ($\sim$ 10 ps) with a high power ($\approx$ 90 TW), approaching the expected requirements for fast ignition [13]. Proton probing [21]

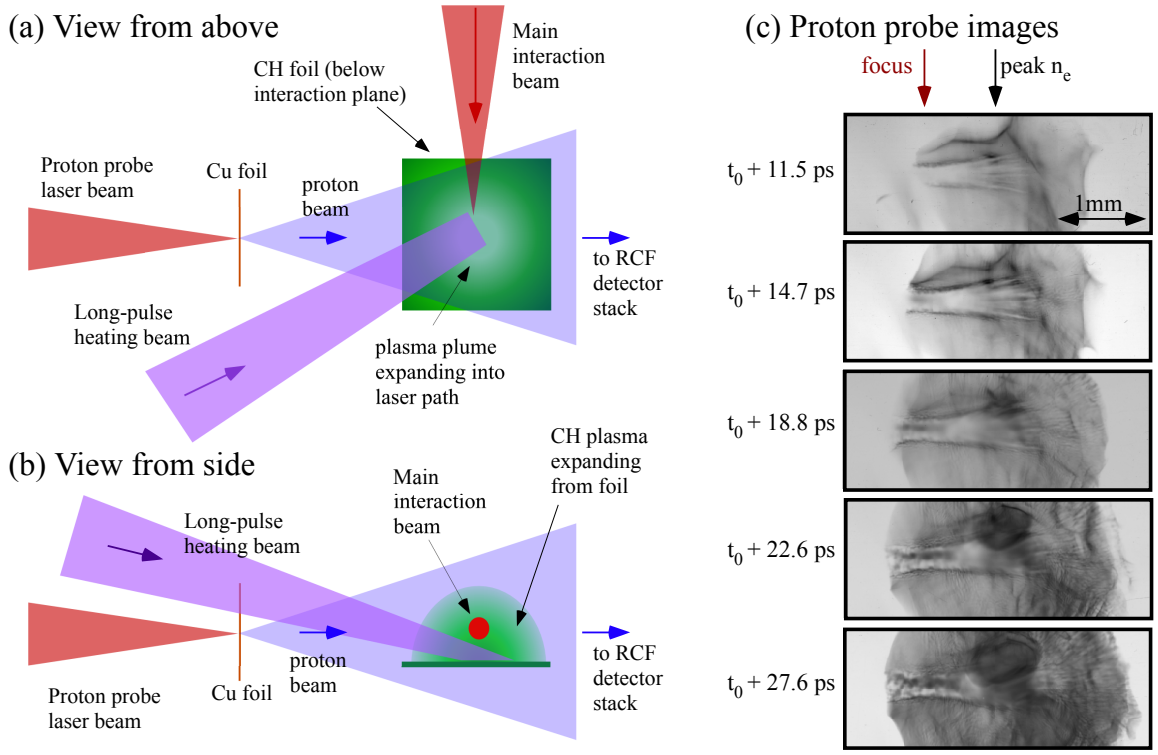

Figure 1. Schematic of the experimental configuration for the proton radiography of the underdense plasma interaction: (a) the view from above and (b) the view from the side. (c) Proton probe images showing a sequence times with the laser pulse traveling from left to right. The contrast of the images has been adjusted to show the features.

was used to image channel formation through underdense plasma [22, 23]. This paper presents additional data from the experiments described in references [19, 24], where the evolution of the electromagnetic fields in the channel was measured using proton radiography. Specifically, we consider the channel radius as a function of time.

2. Experimental set-up

The experiment was performed at the Laboratory for Laser Energetics using the Omega EP laser system. A single long-pulse laser was used to create an underdense plasma target. Two short-pulse beams provided the main interaction pulse and a pulse to generate a proton probe beam. A schematic showing the experimental configuration is shown in figure 1 with views both (a) from above and (b) from the side. The long-pulse beam (2.5 ns duration, wavelength of 351 nm (3ω), 1160 ± 110 J energy, 800 μm diameter focal spot) generated a plasma plume from a planar plastic (CH) target. The two-dimensional hydrodynamic code SAGE [25] determined the plasma electron density profile along the main interaction pulse propagation path to be approximately gaussian (half-width = 650 μm) with a peak plasma density of $n_e = (5 \pm 1) \times 10^{19}$ cm^{-3} (5% of the critical density). The main interaction pulse (8.2 ± 0.4 ps, 743 ± 11 J, giving a pulse power of $\approx$ 90 TW) was focused by an $f/2$ off-axis parabola to a spot where 80% of the energy was contained in a radius of 22 μm. The focal plane was at a density of $n_e = 2.5 \times 10^{19}$ Wcm^{-2}, this was 0.8 mm before the peak density. The peak vacuum intensity was $(2.8 \pm 0.7) \times 10^{19}$ Wcm^{-2}, corresponding to a peak normalized vector potential of $a_0 = 4.7 \pm 0.6$. For creating the proton radiography beam, a third pulse ($\approx$ 0.9 ps, $\approx$ 236 J, wavelength of 1.053 μm) was focused

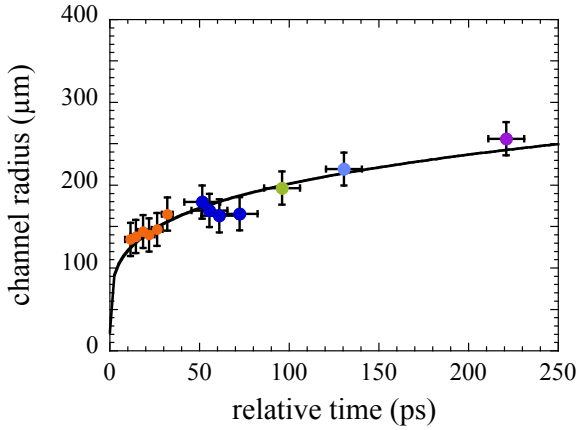

Figure 2. The channel radius as a function of time with the different color markers indicating the different shots used. The line has the function $R = r_0 + \beta t^{\alpha}$.

onto a 50 μm thick copper foil. Target normal sheath acceleration [26] produced an excellent quality probe beam possessing qualities such as a small virtual source size ($\sim$ μm) [27] and good laminarity [28] providing good spatial resolution. The proton generation time was on the order of the laser pulse length ($\sim$ 1 ps) providing good temporal resolution [21]. Since the time it takes the protons to travel from the source foil to the interaction is dependent upon the proton energy, different radiochromic film (RCF) layers will be imaging different times in the interaction, creating an image sequence. To observe different times in the channel evolution, the timing between the main interaction pulse and the proton generating pulse was changed. Further details of the set-up can be found in references [19, 24].

3. Experimental results

Figure 1 (c) shows proton probe images of the channel formation during the interaction. The time, t_0, is defined as when the leading edge of the main interaction pulse reached half-maximum intensity at focus. The strong radial electric fields within the central region deflect the proton probe out of the channel. Examples of channel images from later times are presented in reference [24]. The channel radii from several different shots were analyzed at a position of 300 μm after the focal plane, and are plotted in figure 2. The different shots are illustrated as different marker colors. The fit $R = r_0 + \beta t^{\alpha}$ was made to the experimental data as shown in figure 2, where $r_0 = 22$ μm was assumed to be the focal spot radius and the factors $\beta = 54.6 \pm 5.5$ and $\alpha = 0.26 \pm 0.02$ were determined. Momentum-conservation snowplough models predict $\alpha = 1/3$ for a spherical geometry and $\alpha = 2/5$ for a cylindrical geometry [6]. Therefore the channel expansion was in reasonable agreement with the expected scaling.

In the earliest image, the laser has already propagated a significant distance from the left of the image. But further in to the plasma the channel had broken up into a number of filaments, suggesting that the laser had broken up into several individual filaments [3, 4]. The short focal length parabola ($f/2$) and the imperfect focal spot would assist filamentation. Even though the front of the laser pulse may break up and create a number of individual channels, the pulse was long enough that the excess plasma forming the filamentary channels was expelled by the subsequent part of the laser pulse. Therefore the filaments merge and self-correct into a single channel. This self-correction of the channel has been previously observed in simulations [13]. The filaments merged at a speed of $\approx 0.1c$. A dark region in the center of the channel appears after the initial stages of channel formation and progresses through the channel at a speed of

$\approx 0.12c$, and this likely indicates a region of field inversion inside the channel [22].

4. Summary

In conclusion, proton probing was used to image the interaction of a high-energy, high-power laser pulse through millimeter-scale plasma with a peak density of 5×10^{19} cm^{-3}. The radial channel expansion driven by the ponderomotive potential was in reasonable agreement with the momentum conservation snowplough models [6]. The laser undergoes filamentation, leading to the formation of a number of individual channels. However, providing the laser duration was sustained, the channel eventually self-corrects into a single hollow structure. The finding that filamentation instabilities can be corrected is promising for hole-boring fast ignition schemes.

Acknowledgments

The authors gratefully acknowledge technical assistance from the staff of the Laboratory for Laser Energetics. This material is based upon work supported by the Department of Energy National Nuclear Security Administration under Award Number DE-NA0002028. Work performed by LLNL under the auspices of U.S. DOE under contract DE-AC52-07NA27344.

References

[1] Sprangle P, Tang C-M, and Esarey E 1987 *IEEE Trans. Plas. Sci.* **PS-15**, 145
[2] Borisov A B, Borovskiy A V, Korobkin V V, Prokhorov A M, Rhodes C K, and Shiryaev O B 1990 *Phys. Rev. Lett.* **65**, 1753
[3] Najmudin Z, Krushelnick K, Tatarakis M, Clark E L, Danson C N, Malka V, Neely D, Santala M I K, Dangor A E 2003 *Phys. Plas.* **10**, 438
[4] Nilson P M, *et al.* 2010 *New J. Phys.* **12**, 045014
[5] Forslund D W, Kindel J M, and Lindman E L 1975 *Phys. Fluids* **18**, 1002
[6] Naumova N M, Bulanov S V, Esirkepov T Zh, Farina D, Nishihara K, Pegoraro F, Ruhl H, and Sakharov A S 2001 *Phys. Rev. Lett.* **87**, 185004
[7] Romagnani L, *et al.* 2010 *Phys. Rev. Lett.* **105**, 175002
[8] Borghesi M, MacKinnon A J, Barringer L, Gallard R, Gizzi L A, Meyer C, and Willi O 1997 *Phys. Rev. Lett.* **78**, 879
[9] Sarkisov G S, Bychenkov Yu V, Novikov V N, Tikhonchuk V T, Maksimchuk A, Chen S-Y, Wagner R, Mourou G, and Umstadter D 1999 *Phys. Rev. E* **59** 7042
[10] Burnett N H and Enright G D 1990 *IEEE J. Quant. Elec.* **26**, 1797
[11] Krushelnick K *et al.* 1999 *Phys. Rev. Lett.* **83**, 737
[12] Tabak M, Hammer J, Glinsky M E, Kruer W L, Wilks S C, Woodworth J, Campbell E M, Perry M D, and Mason R J 1994 *Phys. Plas.* **1**, 1626
[13] Li G, Yan R, Ren C, Wang T-L, Tonge J, and Mori W B 2008 *Phys. Rev. Lett.* **100**, 125002
[14] Wei M-S *et al.* 2004 *Phys. Rev. Lett.* **93**, 155003
[15] Nilson P M *et al.* 2009 *Phys. Rev. Lett.* **103**, 255001
[16] Pukhov A, Sheng Z M, and Meyer-ter-Vehn J 1998 *Phys. Rev. Lett.* **5**, 1880
[17] Mangles S P D *et al.* 2005 *Phys. Rev. Lett.* **94**, 245001
[18] Arefiev A V, Breizmann B N, Schollmeier M, and Khudik V N 2012 *Phys. Rev. Lett.* **108**, 145004
[19] Willingale L *et al.* 2013 *New J. Phys.* **15**, 025023
[20] Kneip S *et al.* 2008 *Phys. Rev. Lett.* **100**, 105006
[21] Borghesi M, Schiavi A, Campbell D H, Haines M G, Willi O, Mackinnon A J, Patel P, Galimberti M and Gizzi L A 2003 *Rev. Sci. Inst.* **74**, 1688
[22] Kar S *et al.* 2007 *New J. Phys.* **9**, 402
[23] Sarri G *et al.* 2010 *Phys. Plas.* **17**, 113303
[24] Willingale L *et al.* 2011 *Phys. Rev. Lett.* **106**, 105002
[25] Craxton R S, and McCrory R L 1984 *J. Appl. Phys.* **56**, 108
[26] Hatchett S P *et al.* 2000 *Phys. Plas.* **7**, 2076
[27] Borghesi M, Mackinnon A J, Campbell D H, Hicks D G, Kar S, Patel P K, Price D, Romagnani L, Schiavi A, and Willi O 2004 *Phys. Rev. Lett.* **92** 055003
[28] Cowen T E, *et al.* 2004 *Phys. Rev. Lett.* **92**, 204801
[29] Bulanov S V, Pegoraro F 2002 *Phys. Rev. E* **65**, 066405